Journal of Neuroscience Methods 425 (2026) 110617

Contents lists available at ScienceDirect

Journal of Neuroscience Methods

journal homepage: www.elsevier.com/locate/jneumeth

Short communication

A modified α-synuclein seed amplification assay in Lewy body dementia using Raman spectroscopy and machine learning analysis

Nathan P. Coles [a,b], Suzan Elsheikh [a,b], Alaa Gouda [a,b], Agathe Quesnel [c], Lucy Butler [a,b], Ojodomo J. Achadu [a,b], Meez Islam [a,b], Karunakaran Kalesh [a,b], Annalisa Occhipinti [b,d,e], Claudio Angione [b,d,e], Jon Marles-Wright [f], David J. Koss [g], Alan J. Thomas [h], Tiago F. Outeiro [i,j,k,l], Panagiota S. Filippou [a,b,m], Ahmad A. Khundakar [a,b,i,*]

[a] School of Health & Life Sciences, Teesside University, Middlesbrough TS1 3BX, United Kingdom
[b] National Horizons Centre, Teesside University, Darlington DL1 1HG, United Kingdom
[c] Research Center In Cancer De Toulouse, 2 Av. Hubert Curien, Toulouse 31100, France
[d] School of Computing, Engineering & Digital Technologies, Teesside University, Middlesbrough TS1 3BX, United Kingdom
[e] Centre for Digital Innovation, Teesside University, Middlesbrough TS1 3BX, United Kingdom
[f] Biosciences Institute, Cookson Building, Framlington Place, Newcastle University, Newcastle upon Tyne NE2 4HH, United Kingdom
[g] Division of Neuroscience, School of Medicine, University of Dundee, Nethergate, Dundee, Scotland DD1 4HN, United Kingdom
[h] Newcastle Biomedical Research Centre, Newcastle University, Newcastle upon Tyne NE2 4HH, United Kingdom
[i] Translational and Clinical Research Institute, Faculty of Medical Sciences, Newcastle University, Newcastle upon Tyne United Kingdom
[j] University Medical Center Göttingen, Department of Experimental Neurodegeneration, Center for Biostructural Imaging of Neurodegeneration, Göttingen, Germany
[k] Max Planck Institute for Multidisciplinary Sciences, Göttingen, Germany
[l] Deutsches Zentrum für Neurodegenerative Erkrankungen (DZNE), Göttingen, Germany
[m] Laboratory of Biological Chemistry, School of Medicine, Faculty of Health Sciences, Aristotle University of Thessaloniki, Thessaloniki 54124, Greece

ARTICLE INFO

Keywords:
Lewy body dementia
Raman spectroscopy
α-synuclein aggregation
Machine learning analysis
Diagnostics

ABSTRACT

Background: Lewy body dementias (LBD), comprising dementia with Lewy bodies (DLB) and Parkinson's disease dementia (PDD), are defined by misfolded α-synuclein aggregation. Seed amplification assays (SAAs), such as RT-QuIC, enable sensitive detection of α-synuclein aggregates but typically provide binary readouts and require fluorescence labeling. Raman spectroscopy offers a label-free approach to detect subtle biochemical changes, and its diagnostic potential can be enhanced with machine learning.

Objectives: This proof-of-concept study aimed to evaluate whether Raman spectroscopy combined with machine learning can improve SAA-based discrimination of LBD from controls in cerebrospinal fluid (CSF).

Methods: We analyzed a small number of post-mortem CSF samples from pathologically confirmed DLB (n = 2), PDD (n = 2), and controls (n = 2) using a 7-day SAA. Raman spectra were collected on Days 1, 4, and 7 and analyzed using principal component analysis (PCA) and uniform manifold approximation and projection (UMAP).

Results: Following SAA, both PCA and UMAP distinguished combined LBD samples from controls within 24 h (Day 1), reflecting biochemical changes consistent with α-synuclein fibrillation. Spectral shifts indicated decreased α-helical content with increased β-sheet structures. No consistent separation between DLB and PDD was observed.

Conclusion: This preliminary study demonstrates that combining Raman spectroscopy with machine learning can enable rapid, label-free detection of disease-specific changes. Despite the very limited sample size, these findings highlight the potential of this novel workflow and strongly warrant its validation in larger cohorts.

* Corresponding author at: School of Health & Life Sciences, Teesside University, Middlesbrough TS1 3BX, United Kingdom.
E-mail address: a.khundakar@tees.ac.uk (A.A. Khundakar).

https://doi.org/10.1016/j.jneumeth.2025.110617
Received 24 September 2025; Received in revised form 21 October 2025; Accepted 2 November 2025
Available online 12 November 2025

1. Introduction

Lewy body dementias (LBD), including Parkinson's disease dementia (PDD) and dementia with Lewy bodies (DLB), are progressive neurodegenerative disorders linked to the misfolding and aggregation of α-synuclein protein (Outeiro et al., 2019; Spillantini et al., 1998). The misfolded α-synuclein protein is thought to spread in a prion-like manner, leading to widespread neuronal damage and clinical symptoms of dementia (Brundin and Melki, 2017). α-synuclein seed amplification assays (SAAs), such as real-time quaking-induced conversion (RT-QuIC) and protein misfolding cyclic amplification (PMCA), rely on the self-propagation of misfolded α-synuclein aggregates, enabling sensitive in vitro detection of disease-related protein biomarkers. These assays have shown considerable promise in identifying α-synuclein aggregates in biofluid samples like cerebrospinal fluid (CSF) (Concha-Marambio et al., 2023) and more recently blood (Okuzumi et al., 2023), offering a potentially reliable pre-mortem diagnostic tool in LBD. However, SAAs do possess limitations. For instance, the RT-QuIC assay typically categorizes both conditions under a single binary outcome, overlooking their distinct pathophysiological differences and limiting its capacity to capture the nuances of LBD, as well as the necessity for thioflavin T binding and fluorescence detection. In contrast, Raman spectroscopy is a label-free technique that analyzes light scattering to produce molecular fingerprints, allowing the detection of a wide range of subtle biochemical changes in samples without the use of dyes (Butler et al., 2016). Recent advancements in machine learning have further enhanced the diagnostic potential of Raman spectroscopy, as demonstrated in disease diagnostics studies (Quesnel et al., 2023). In this preliminary proof-of-concept study, we aim to explore the diagnostic utility of combining Raman spectroscopy with machine learning in a small number of post-mortem CSF samples from patients with DLB, PDD and age-matched controls. While current diagnostic criteria are effective for established dementia, there remains a clear need for more sensitive, biological tools to enable early and differential diagnosis. Our platform aims to address this gap by providing a rapid, label-free method that generates rich biochemical data beyond a simple binary outcome. Establishing this capability lays a critical foundation for future large-scale studies, such as those aimed at differentiating LBD from Alzheimer's disease (AD) or identifying individuals with prodromal LBD, such as REM sleep behaviour disorder.

2. Methods

Post-mortem CSF samples were obtained from a small cohort of patients with pathologically categorized DLB (n = 2), PDD (n = 2), and age-matched controls (n = 2) from the Newcastle Brain Tissue Resource. This minimal sample size was selected for an initial proof-of-concept investigation. Ethical approval for use of the CSF samples was obtained from Newcastle University and the Newcastle and North Tyneside Health Authority. The control patients, aged 88 and 80, exhibited no Lewy body pathology and had high Mini-Mental State Examination (MMSE) scores of 26 and 30. The PDD patients, both aged 82, demonstrated high Braak PD stage (6), with neocortical Lewy body pathology and had MMSE scores of 13 and 17, respectively. The DLB patients, aged 81 and 79, also had high Braak PD stage (6) and neocortical Lewy body pathology, with MMSE scores of 14 and 4, respectively. CSF was collected immediately after post-mortem, centrifuged to remove any blood contamination and stored at –80°C. All cases underwent clinical assessments during life and neuropathological diagnosis confirmed. Human wildtype α-synuclein was produced and purified using an *Escherichia coli (E. coli)* expression system. Transfection of *E. coli* BL21 (DE3) cells with pCDNA3.1-asyn plasmid (provided by Outeiro lab) was used for protein overexpression after induction with IPTG (1 mM) at 37 °C. The cells were lysed, and the protein was purified via ion-exchange and size-exclusion chromatography, as described elsewhere (Coles et al., 2024b). To conduct the SAA, 100 μL of CSF from each sample was mixed with 100 μL of 0.1 mg/mL monomeric α-synuclein in a low-salt buffer. The mixture was incubated with glass beads at 37°C and agitated at 1000 rpm for 7 days. Samples were collected at 3 time points: Day 1 (D)1, D4, and D7, then analyzed using Raman spectroscopy. Raman spectra were acquired using an inVia™ confocal Raman microscope (Renishaw, Gloucestershire, UK) with a 785 nm laser. For each sample, 5 spectra were recorded and processed to remove cosmic rays and perform baseline correction. The data were normalized using standard normal variate (SNV) transformation and analyzed with principal component analysis (PCA) to visualize the most significant group spectral variations. Uniform manifold approximation and projection (UMAP) analysis was also performed to analyze non-linear group separation.

3. Results

PCA and UMAP analyses were used to visually analyze spectral differences between the groups, testing for both linear and nonlinear relationships among variables. Without SAA induction, neither PCA nor UMAP could differentiate between disease and control CSF samples, suggesting that signal amplification is necessary for discrimination. However, after SAA induction, and despite the small group sizes, both PCA and UMAP analyses differentiated DLB and PDD samples from controls at D1, confirming early-stage biochemical changes in the disease groups (Fig. 1, A and B). UMAP plots for D1 revealed clear separation between disease and control samples, though not between disease groups, with Random Forest analysis (100 trees, 10-fold cross-validation) classifying D1 samples with 73 % accuracy ($\kappa = 0.6$). This accuracy declined to 23 % and 50 % for D4 and D7, respectively, consistent with increasing spectral variability over time. This delineation within 24 h demonstrates the ability to rapidly detect a multivariate spectral signature of disease, far sooner than the fluorescence readout of traditional RT-QuIC. PCA and UMAP analysis of Raman spectra could not detect differences between the disease groups (DLB and PDD) at any time point. 10 of the 20 influential wavenumbers identified from the spectra exhibited intensity changes in disease groups, primarily reflecting α-synuclein aggregation (Fig. 1, C). Increase in C-C-C bonds (802 cm^{-1}) was found, indicative of protein-protein interactions, along with a decrease in α-helical structures (1341 cm^{-1}, 1657 cm^{-1}, 1718 cm^{-1}) and concurrent increase in β-sheet structures (1493 cm^{-1}, 1625 cm^{-1}) (Ettah and Ashton, 2018; Girard et al., 2021; Palombo et al., 2018; Pezzotti, 2021; Webster et al., 2011). Additionally, alterations in specific amino acids were observed, including reduced tyrosine-related intensities (805 cm^{-1}) and increased phenylalanine levels (1005 cm^{-1}) in PDD samples at D1 (Maiti et al., 2004; Pezzotti, 2021). These changes suggest rapid structural modifications linked to α-synuclein fibrillation after SAA initiation. However, no distinction in spectral variability was observed between the disease groups (DLB and PDD) and the age-matched controls at D4 or D7.

4. Discussion

In this proof-of-concept study, a modified SAA was combined with Raman spectroscopy and machine learning to analyze post-mortem CSF samples from a limited number of patients with DLB and PDD compared to controls. PCA and UMAP analysis revealed clear distinctions between the disease and control groups at day 1 of the assay, but not at days 4 or 7, and no separation between the DLB and PDD groups was detected at any time point. This suggests that the most significant biomolecular changes occurred early in the assay, driven by the introduction of monomeric recombinant wild-type α-synuclein, which promoted the transition from α-helical to β-sheet structures, mirroring typical α-synuclein fibrillation spectral patterns we recently found in purified recombinant protein samples (Coles et al., 2024b) and cell lines (Coles et al., 2024a). The primary innovation of this study is the synergistic integration of SAA, Raman spectroscopy and PCA/UMAP analysis into a

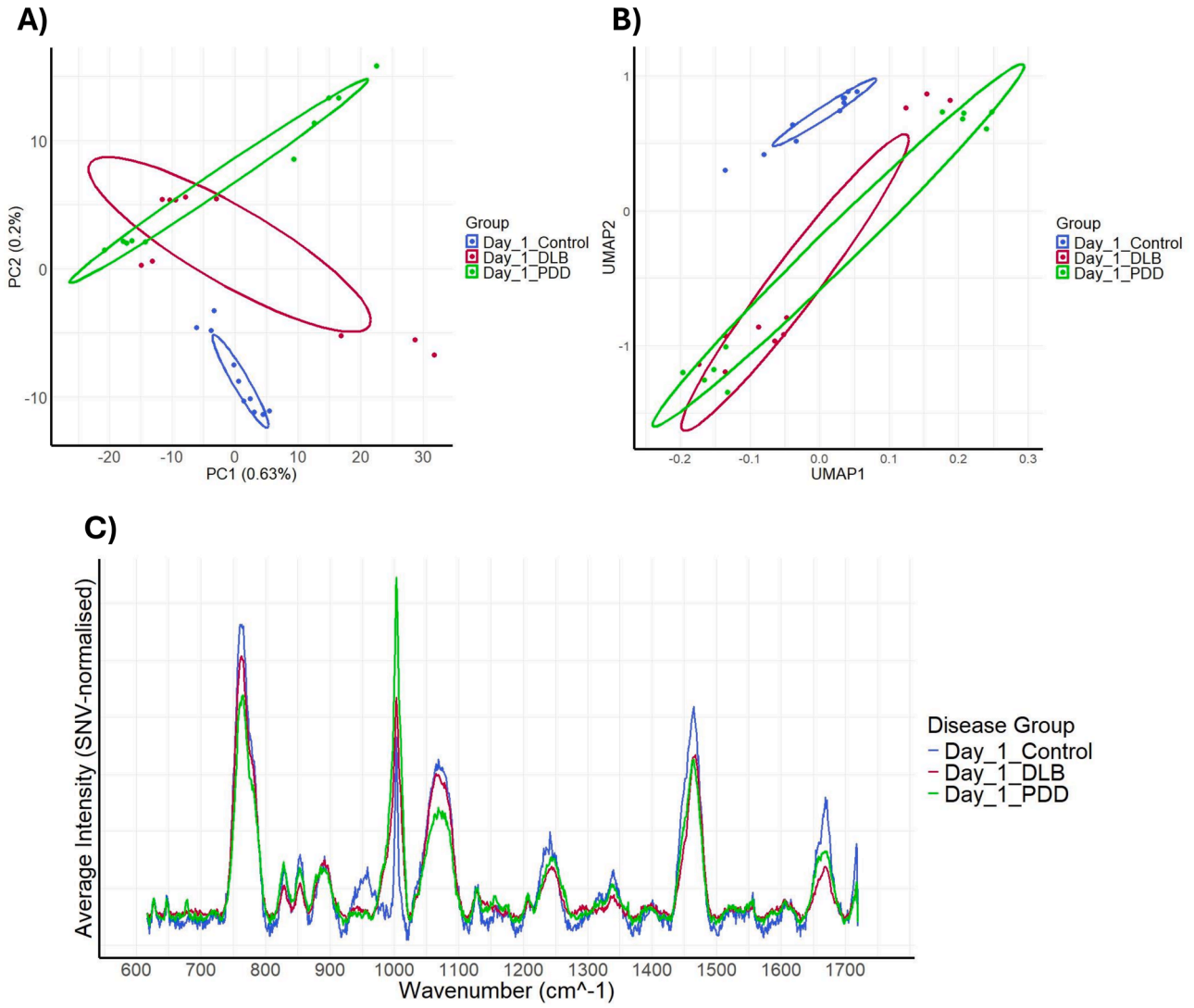

Fig. 1. A) PCA plot for D1 (early stage) of the modified SAA. **B)** UMAP plot for D1 of the modified SAA. Both plots reveal clear delineation between CSF disease (DLB and PDD) and control group. C) Ten wavenumbers which showed statistically significant changes in disease groups when compared to the control group. Most of the changes were found on D1, with two found on D4 and no changes found on D7. **D)** Spectral overlay for D1, showing average peak intensities, which were identified through unbiased machine learning and visual analysis to assess significant spectral differences.

single workflow in the diagnosis of LBD. We demonstrate that this platform can rapidly decode the biochemical process of aggregation, providing a rich, multivariate profile that surpasses the binary 'yes/no' result of standard seed amplification assays

Despite the small sample size (n = 2 per group), the combination of Raman spectroscopy and machine learning shows initial promise as a diagnostic tool for differentiating control from LBD samples after SAA induction. PCA and UMAP analyses of this spectral information distinguished control CSF from both DLB and PDD CSF at D1 following SAA induction, demonstrating the potential ability to detect early biochemical changes. This approach could potentially thus provide a more efficient differentiation between disease and control samples compared to traditional assays like RT-QuIC, which typically require several days to detect protein misfolding patterns.

At D1, 10 spectral peaks displayed significant intensity changes in the DLB and PDD groups compared to controls, reflecting rapid α-synuclein fibrillation. There was a marked decrease in α-helical-associated peaks and a concurrent increase in β-sheet-associated peaks in the disease groups, indicative of transition in α-synuclein from a soluble state to insoluble fibrils. Specifically, peaks related to amide I and III bonds, associated with α-helical structures, decreased in the disease groups, suggesting a loss of α-synuclein tetramers (Coles et al., 2024b; Ettah and Ashton, 2018; Spedalieri et al., 2023; Webster et al., 2011). In contrast, β-sheet-associated peaks increased, reflecting the recruitment of monomeric α-synuclein into β-sheet-rich aggregates (Coles et al., 2024b; Maiti et al., 2004; Pezzotti, 2021). Additionally, a reduction in tyrosine-related peaks (805 cm^{-1}) was found in DLB samples, consistent with tyrosine involvement in early fibril formation. Tyrosine residues significantly influence α-synuclein aggregation, with specific regions acting differently based on protein conformation (Ruf et al., 2008). Aggregation of α-synuclein begins with the interaction of C-terminal region tyrosines, initially limited by a compact structure (Ruf et al., 2008). Without an N-terminal region tyrosine (e.g., Tyr39), aggregation progresses from dimers to larger aggregates like tetramers and hexamers (Palomino-Hernandez et al., 2020; Zamel et al., 2023). Crosslinking promotes nucleation, stabilizing dimers as precursors for oligomers. Thus, the diminished vibrational activity of tyrosine peaks suggests that tyrosine residues become less accessible as they integrate into fibrils through intermolecular interactions. However, an increase in phenylalanine levels (1005 cm^{-1}) was observed in PDD samples at D1, suggesting a role in stabilizing β-sheet-rich aggregates. This transition emphasizes the critical role of hydrophobic and aromatic residues, like

phenylalanine, in stabilizing fibrils with cross-seeding potential (Ramesh et al., 2013). Such subtle differences in amino acid changes between DLB and PDD samples may indicate the amplification of distinct α-synuclein strains (Kannarkat et al., 2024; Van der Perren et al., 2020), which could manifest as phenotypic variations in the Raman spectra. However, these interpretations are based on a very small number of samples and further investigation in a larger patient cohort is necessary to confirm these findings and to fully elucidate the molecular mechanisms underlying these differences. The absence of significant differences between LBD and control groups at D4 and D7 suggests that disease-specific spectral changes occur early in the aggregation process. Later time points may represent a converged fibrillation endpoint or sample degradation, highlighting the importance of early-phase measurements for diagnostic accuracy.

We acknowledge the limitations of this study. Post-mortem samples are influenced by factors such as agonal state, post-mortem interval, and autolysis, which can alter protein and metabolite profiles and complicate the translation of findings to clinical settings (Ranganathan et al., 2007). Moreover, as more dementia diagnoses are made in mental health than in neurology settings, where routine CSF analysis is often unavailable, this may further limit the generalisability and clinical translation of our findings. To establish the diagnostic utility of this approach in people living with dementia, it will be essential to validate the assay using ante-mortem CSF, standardize collection and handling protocols, and ensure reproducibility across laboratories. Future studies could also address a key clinical challenge by determining whether Raman spectroscopy can detect distinct spectral profiles that differentiate co-morbid pathologies, such as overlapping synucleinopathies and Aβ/tau proteinopathies, thereby improving diagnostic precision between neurodegenerative diseases like AD and LBD. Extending this approach to prodromal cohorts, including individuals with REM sleep behaviour disorder, will further assess its potential as an early, biologically based diagnostic tool for LBD. Incorporating a labelled approach, such as surface-enhanced Raman spectroscopy (SERS), in future research could further enhance detection sensitivity by amplifying specific molecular signals associated with disease markers.

Overall, our proof-of-concept approach demonstrates the potential of combining Raman spectroscopy with machine learning to advance SAA-based diagnostics in LBD and justifies more extensive validation in larger, more diverse cohorts, including patients with AD and prodromal disorders.

CRediT authorship contribution statement

Claudio Angione: Writing – review & editing, Writing – original draft, Validation, Software, Formal analysis. **David J. Koss:** Writing – review & editing, Methodology. **Nathan P. Coles:** Writing – review & editing, Writing – original draft, Visualization, Validation, Investigation, Formal analysis. **Jon Marles-Wright:** Writing – review & editing, Methodology. **Tiago F. Outeiro:** Writing – review & editing, Supervision, Resources, Methodology, Conceptualization. **Alaa Gouda:** Writing – review & editing. **Alan J. Thomas:** Writing – review & editing, Methodology. **Suzan Elsheikh:** Writing – review & editing, Validation, Formal analysis. **Ahmad A. Khundakar:** Writing – review & editing, Writing – original draft, Supervision, Project administration, Methodology, Investigation, Formal analysis, Conceptualization. **Lucy Butler:** Writing – review & editing, Validation. **Panagiota S. Filippou:** Writing – review & editing, Writing – original draft, Validation, Supervision, Project administration, Methodology, Formal analysis, Conceptualization. **Agathe Quesnel:** Writing – review & editing, Validation. **Meez Islam:** Writing – review & editing. **Ojodomo J. Achadu:** Writing – review & editing, Writing – original draft, Methodology. **Annalisa Occhipinti:** Writing – review & editing, Writing – original draft, Validation, Software, Conceptualization. **Karunakaran Kalesh:** Writing – review & editing, Writing – original draft.

Funding sources

This research did not receive any specific grant from funding agencies in the public, commercial, or not-for-profit sectors.

Declaration of Competing Interest

The authors declare that they have no known competing financial interests or personal relationships that could have appeared to influence the work reported in this paper.

Acknowledgements

We extend our thanks to Debbie Lett, along with other staff at the Newcastle Brain Tissue Resource, Newcastle University, for their valuable support and to the patients and their families who generously donated the CSF samples for this research. Additionally, we thank the staff at the National Horizons Centre, Teesside University, for their technical support and advice.

Data availability

The codes generated and analyzed during the current study are openly available in the GitHub repository at https://github.com/NColes2812/RamanSpectralAnalysis

References

Brundin, P., Melki, R., 2017. Prying into the Prion Hypothesis for Parkinson's Disease. J. Neurosci. 37, 9808–9818.

Butler, H.J., Ashton, L., Bird, B., Cinque, G., Curtis, K., Dorney, J., Esmonde-White, K., Fullwood, N.J., Gardner, B., Martin-Hirsch, P.L., Walsh, M.J., McAinsh, M.R., Stone, N., Martin, F.L., 2016. Using Raman spectroscopy to characterize biological materials. Nat. Protoc. 11, 664–687.

Coles, N.P., Elsheikh, S., Butler, L., Jennings, C., Marles-Wright, J., Achadu, O., Islam, M., Koss, D., Occhipinti, A., Angione, C., Thomas, A.J., Outeiro, T.F., Filippou, P.S., Khundakar, A.A., 2024b. Molecular Insights into α-Synuclein Fibrillation: A Raman Spectroscopy and Machine Learning Approach. Under Review.

Coles N.P., Elsheikh, S., Butler, L., Achadu, O., Kalesh, K., Islam, M., Occhipinti, A., Angione, C., Marles-Wright, J., Koss, D.J., Thomas, A.J., Outeiro, T.F., Filippou, P.S., & Khundakar, A.A. Prominent cellular lipid changes during α-synuclein aggregation revealed by Raman spectroscopy and machine learning analysis, 2024a.

Concha-Marambio, L., Pritzkow, S., Shahnawaz, M., Farris, C.M., Soto, C., 2023. Seed amplification assay for the detection of pathologic alpha-synuclein aggregates in cerebrospinal fluid. Nat. Protoc. 18, 1179–1196.

Ettah, I., Ashton, L., 2018. Engaging with Raman spectroscopy to investigate antibody aggregation. Antibodies (Basel) 7.

Girard, A., Cooper, A., Mabbott, S., Bradley, B., Asiala, S., Jamieson, L., Clucas, C., Capewell, P., Marchesi, F., Gibbins, M.P., Hentzschel, F., Marti, M., Quintana, J.F., Garside, P., Faulds, K., MacLeod, A., Graham, D., 2021. Raman spectroscopic analysis of skin as a diagnostic tool for Human African Trypanosomiasis. PLOS Pathog. 17. : e1010060-e1010060.

Kannarkat, G.T., Zack, R., Skrinak, R.T., Morley, J.F., Davila-Rivera, R., Arezoumandan, S., Dorfmann, K., Luk, K., Wolk, D.A., Weintraub, D., Tropea, T.F., Lee, E.B., Xie, S.X., Chandrasekaran, G., Lee, V.M., Irwin, D., Akhtar, R.S., Chen-Plotkin, A.S., 2024. α-synuclein conformations in plasma distinguish parkinson's disease from dementia with Lewy bodies. Res Sq.

Maiti, N.C., Apetri, M.M., Zagorski, M.G., Carey, P.R., Anderson, V.E., 2004. Raman spectroscopic characterization of secondary structure in natively unfolded proteins: α-synuclein. J. Am. Chem. Soc. 126, 2399–2408.

Okuzumi, A., Hatano, T., Matsumoto, G., Nojiri, S., Ueno, S.I., Imamichi-Tatano, Y., Kimura, H., Kakuta, S., Kondo, A., Fukuhara, T., Li, Y., Funayama, M., Saiki, S., Taniguchi, D., Tsunemi, T., McIntyre, D., Gerardy, J.J., Mittelbronn, M., Kruger, R., Uchiyama, Y., Nukina, N., Hattori, N., 2023. Propagative alpha-synuclein seeds as serum biomarkers for synucleinopathies. Nat. Med. 29, 1448–1455.

Outeiro, T.F., Koss, D.J., Erskine, D., Walker, L., Kurzawa-Akanbi, M., Burn, D., Donaghy, P., Morris, C., Taylor, J.-P., Thomas, A., Attems, J., McKeith, I., 2019. Dementia with Lewy bodies: an update and outlook. Mol. Neurodegener. 14, 5.

Palombo, F., Tamagnini, F., Jeynes, J.C.G., Mattana, S., Swift, I., Nallala, J., Hancock, J., Brown, J.T., Randall, A.D., Stone, N., 2018. Detection of Aβ plaque-associated astrogliosis in Alzheimer's disease brain by spectroscopic imaging and immunohistochemistry. Analyst 143, 850–857.

Palomino-Hernandez, O., Buratti, F.A., Sacco, P.S., Rossetti, G., Carloni, P., Fernandez, C. O., 2020. Role of Tyr-39 for the structural features of alpha-synuclein and for the interaction with a strong modulator of its amyloid assembly. Int. J. Mol. Sci. 21.

Pezzotti, G., 2021. Raman spectroscopy in cell biology and microbiology. J. Raman Spectrosc. 52, 2348–2443.

Quesnel, A., Coles, N., Angione, C., Dey, P., Polvikoski, T.M., Outeiro, T.F., Islam, M., Khundakar, A.A., Filippou, P.S., 2023. Glycosylation spectral signatures for glioma grade discrimination using Raman spectroscopy. BMC Cancer 23, 174.
Ramesh, J., Srinivasan, S., Ramkumaar, G., 2013. Molecular structure, vibrational spectra, UV–vis, NBO, and NMR analyses on nevirapine using ab initio DFT methods. J. Theor. Appl. Phys. 7, 51.
Ranganathan, S., Nicholl, G.C., Henry, S., Lutka, F., Sathanoori, R., Lacomis, D., Bowser, R., 2007. Comparative proteomic profiling of cerebrospinal fluid between living and post mortem ALS and control subjects. Amyotroph. Lateral Scler. 8, 373–379.
Ruf, R.A.S., Lutz, E.A., Zigoneanu, I.G., Pielak, G.J., 2008. α-synuclein conformation affects its tyrosine-dependent oxidative aggregation. Biochemistry 47, 13604–13609.
Spedalieri, C., Plaickner, J., Speiser, E., Esser, N., Kneipp, J., 2023. Ultraviolet resonance Raman spectra of serum albumins. Appl. Spectrosc. 77, 1044–1052.
Spillantini, M.G., Crowther, R.A., Jakes, R., Hasegawa, M., Goedert, M., 1998. alpha-Synuclein in filamentous inclusions of Lewy bodies from Parkinson's disease and dementia with lewy bodies. Proc. Natl. Acad. Sci. USA 95, 6469–6473.
Van der Perren, A., Gelders, G., Fenyi, A., Bousset, L., Brito, F., Peelaerts, W., Van den Haute, C., Gentleman, S., Melki, R., Baekelandt, V., 2020. The structural differences between patient-derived α-synuclein strains dictate characteristics of Parkinson's disease, multiple system atrophy and dementia with Lewy bodies. Acta Neuropathol. 139, 977–1000.
Webster, G.T., Dusting, J., Balabani, S., Blanch, E.W., 2011. Detecting the early onset of shear-induced fibril formation of insulin in situ. J. Phys. Chem. B 115, 2617–2626.
Zamel, J., Chen, J., Zaer, S., Harris, P.D., Drori, P., Lebendiker, M., Kalisman, N., Dokholyan, N.V., Lerner, E., 2023. Structural and dynamic insights into alpha-synuclein dimer conformations. Structure 31, 411–423 e6.